Electrochemical Impedance Spectroscopy of Battery Systems, including Sodium Materials

Renjie Liu, Derek C Sinclair and Anthony R West

University of Sheffield,

School of Chemical, Materials and Biological Engineering,

Mappin St,

Sheffield S1 3JD, UK

Abstract

An overview is given of the literature on current approaches to the measurement, analysis and interpretation of broadband impedance data and examples of its application to Na materials, cells and batteries. Standard 2-terminal measurements on full cells are often complemented by both 2- and 3-terminal measurements on a range of materials and cell configurations; this should enable identification of the different impedance contributions that control full cell operation. Data analysis usually revolves around equivalent circuit modelling; strategies to identify the most appropriate circuits are reviewed, including increasing use of the distribution of relaxation times methodology. Interfacial phenomena are fundamental components of solid electrolyte interfaces and composite electrodes in operational batteries; these are reviewed for Na-based materials and systems.

Introduction

Batteries are complex systems that have numerous contributions to their overall impedance, many of which change during cycling. Electrochemical impedance spectroscopy (EIS) is of growing importance for the characterisation of operando electrochemical systems, facilitated by the diversification of measurement and analysis procedures. Most methodologies use broadband data collected in the frequency domain that routinely, permit measurements over at least ten decades of frequency. Equivalent circuit modelling (ECM) of the impedance response depends on the availability of high-quality broadband data for two reasons. First, in order to deconvolute the contributions of impedances that overlap on the frequency scale, each of which consists of broadband data rather than fixed frequency resonances, it is necessary to have data that cover several decades of frequency. This is because EIS is a relaxation spectroscopy and not one of the many examples of fixed frequency resonance spectroscopy. Second, in order to recognise and model non-ideality in impedance data that may be linked to diffusion processes, which also have a characteristic frequency dependence, data covering several decades of frequency are again needed. Here we summarise the state of the art in impedance analysis of electrochemical materials and systems in general and then review specifically, current advances in Na-based systems.

Experimental methodology of EIS

The perennial problem in recording, analysing and interpreting 2-terminal impedance data from full-cell configurations is overlap on the frequency scale of separate contributions from the two electrode-electrolyte interface regions. Approaches to separate these components include: (i) measurements on half cells that have been prepared to contain either the cathode or the anode interface with the electrolyte, but noting also that the impedance of the Na counter electrode / electrolyte interface that is also present in the cell may contribute significantly to the overall impedance; (ii) measurements of symmetric cells that consist of two identical working electrodes at the same state of charge. This often requires recovering two electrodes (either both positive side or both negative side) from two cycled cells, and reassembling them as a new cell. In principle, the specific electrode impedance in the original half cells should equal half of the overall impedance of the symmetric cell [1]. This procedure allows the analysis of single electrode impedance interfaces, but involves possible complications associated with cell disassembly and reassembly processes that may weaken the validity of the resulting impedance data; (iii) less frequently, 3-terminal measurements that involve a third, spectator electrode which allows the two electrode-electrolyte interfaces in a full cell to be studied in separate two terminal measurements.

One of the perceived difficulties involved in 3-terminal measurements is uncertainty over the effect of electrode configuration (their geometry, location and separation) on the lines of force between different electrode pairs and the subsequent analysis of impedance data. In one case using finite-element simulations, it was shown that a combination of electrode misalignment and using electrodes of different nature can disturb the potential of a reference electrode, especially when the electrolyte resistance is large [2]. In an experimental study it was shown that, with the Na metal reference electrode sandwiched between two separators and located above the electrode stack, the sum of the separate 2-terminal electrode responses was equal to that of overall 2-terminal impedance data from the same cell [3,4], Fig.1. The influence of surface cracks and voids on impedance data of homogeneous materials has been assessed by finite element modelling [5] as well as spreading resistances associated with different electrode configurations [6]. Diffusion through porous electrodes leads to complications in modelling the electrochemical processes and choice of most appropriate ECM; this has been treated by introduction of an electrode tortuosity factor [7,8].

For cells with low apparent resistance, such as batteries, inductances frequently occur at high frequencies as an extended ‘hook’ in the fourth quadrant of the impedance complex plane plots. This behaviour is usually associated with either the instrument connection or the sample measuring set-up. Inductive artifacts can also arise in the low-frequency region due to nonlinear responses in conductive systems [9]. For instance, in an EIS measurement of graphite anode [10] and in a theoretical analysis

of metal dissolution reactions [11], both performed under oxidation conditions, the low-frequency inductive loops were consistently ascribed to the combined effects of charge transfer and ion diffusion. Notably, the inductive behaviour disappeared when the diffusion current density had stabilised, to give a linear response. It is also necessary to be aware of stray capacitances in impedance measurements and the importance of cell design. An example value of a stray capacitance is 10 pF in a 2032-type coin cell [12].

Data analysis strategies

Data analysis strategies, especially for higher frequency data on individual materials components, are frequently based on ECMs that consist of series-connected impedances. This is supported by the generation of realistic values of fitted resistance and capacitance parameters. The use of either impedance spectroscopy (IS) or dielectric spectroscopy (DS) approaches to data analysis can lead to the same conclusions. This is because, for a particular ECM, the *R*-*C* elements that are identified are parallel-connected for IS and series-connected for DS [13], and both types of element can be identified in a typical ECM. The time constants, τ, associated with each *R*-*C* element, given by $\tau = RC$, occur at different frequencies, f, given by $2\pi f\tau = 1$ and therefore, different time constants are identified in IS and DS analyses. The data collection procedures are in principle the same for IS and DS but the techniques differ in the analysis of the datasets and choice of *R*-*C* elements that are considered.

A widely-used approach to analysis of impedance data involves complex non-linear least squares (CNLS) fitting but this relies on the availability of an ECM [14]. The fundamental element for conductive materials is taken to be the parallel *R*-*C* element, usually modified to be a parallel *R*-*C*-*CPE* element, in which the constant phase element (CPE) component is added to represent departures from ideality. Commercially-available software may simplify the parallel element to *R*-*CPE*, but exclusion of the limiting high frequency capacitance C_∞ of a material component can lead to erroneous results, especially at high frequencies [15]. This is because the frequency-dependence of a CPE changes continuously unless and until it is terminated in an ECM by inclusion of a frequency-independent resistance at low frequencies and a frequency-independent capacitance at high frequencies. A further practical complication arises if the overall circuit contains more than one CPE, each of which makes a significant contribution to the overall impedance over a wide frequency range; it may then be impossible to arrive at a unique solution and set of parameter values during fitting procedures.

For most ECMs, it is usually assumed that the fundamental parallel elements, whether they are *R*-*C*, *R*-*C*-*CPE*, or *R*-*CPE*, are connected in series, especially for solid materials that may have series-connected current pathways through bulk, grain boundary and surface layer components. Some ECMs may require additional parallel-

connected components in systems where (i) dielectric processes occur in parallel with long range conduction [13], (ii) mixed conductors have independent ionic and electronic conduction (MIEC), (iii) electrode processes have different contributing impedances to the overall response or (iv) porous electrodes present alternative conduction pathways. In the last case, detailed analysis of the impedance may involve transmission line models (TLMs) [16,17]. Fig.2(a)(b) shows a TLM of a porous insertion battery electrode and its physical origins [16]. Choice of which ECM to use may be ambiguous because always, multiple ECMs can fit experimental datasets. Insights into the most appropriate ECM can often be obtained by varying experimental parameters such as temperature, oxygen partial pressure, applied dc bias, processing conditions to control microstructure, electrode materials and dopant type or concentration. As yet, there is no a priori method to determine what is the most appropriate ECM for a given dataset.

Impedance data that include electrochemical reactions and diffusion elements have led to the inclusion of *E* in the now widely-adopted EIS terminology, although the terms EIS and IS are fully interchangeable. The Randles circuit element is commonly used for interpretation of electrode processes but complications arise when inclusion of frequency-dependent Warburg diffusion elements, *W*, is necessary [18]. This has led to two widely-used circuit components in which the Warburg is either an integral part of the charge transfer reaction, as in the Randles circuit, or is a separate diffusion impedance that is decoupled from the charge transfer process, Fig.2(c). From Randles' intention to solve the diffusion processes, the Warburg element should not be taken as an independent element because the diffusion resistance and charge transfer resistance are both influenced by interfacial concentration of reacting species [19]. However, there is an increasing trend in the battery literature to decouple the Warburg diffusion element from the charge transfer process, especially when the frequency domains are well separated [18].

The semi-infinite Warburg is a special case of a CPE with a power order, 'n' or 'α', of 0.5. CPEs with different orders are also a ubiquitous presence in high frequency bulk IS data, especially for many well-studied ionic conductors. Ideal, Debye-like behaviour with single relaxation times is rarely observed in practice since cooperative interactions between conducting species are invariably present. These lead to *R* and *C* components that are frequency-dependent. Earlier studies of departures from ideality were often fitted to empirical distributions of relaxation times (DRTs), or especially and more recently, to Jonscher's law of Universal Dielectric Response (UDR) [20]. Quantitative interpretation of the non-ideality and significance of the Jonscher 'n' parameter was not part of accepted wisdom until Almond and coworkers [21] made the link between Jonscher power law behaviour, the value of the 'n' parameter and ECMs. They showed that 'n' was a direct measure of the number of series- and parallel-connected *R*-*C* elements that were modelled in network circuits containing a

very large number of *R* and *C* components, and was supported by experimental data from two-phase composites of dielectrics and ionic conductors [22].

An alternative approach to IS data analysis that makes no *a priori* assumptions about equivalent circuits, involves deconvolution of data sets into a number of individual relaxation times. The resulting DRT profile can, in principle, be related to individual electrochemical processes [23,24]. In one case, it was suggested that DRT peaks, and how they evolve during cycling of Lithium-ion batteries (LIBs), can be related to ageing mechanisms and performance decline [25]. However, it has also been shown that DRTs may give extra peaks and incorrect *R* values when compared with the results of CNLS, especially if inductances are present in the ECM [26].

The term DRT now has two meanings in the literature. There is a vital difference between the concepts of (i) a collection of non-interacting, individual, ideal relaxation times, as in current use of DRT terminology for the analysis of electrochemical impedance data and (ii) the more historical use of a distribution of relaxation times, represented by various functions such as Cole-Davidson or Jonscher power law to include non-ideality, within a single electrochemical process, such as ionic conduction in alkali silicate glasses. It remains to be seen whether the unavoidable non-ideality in experimental datasets, represented by CPEs in ECMs can be treated by DRTs in which each DRT is made up of a number of separate ideal *RC* elements. This new approach to DRTs is certainly an interesting development, but as yet, is not poised to replace more traditional ECM analysis which can in principle give quantitative data fitting and interpretation based on Almond's analysis.

Another approach to non-ideality in EIS, which is regarded as an integral characteristic of electrochemical systems, is to consider effects associated with dynamical processes, especially in operational batteries [27]. These include (i) solid-state diffusion, (ii) intercalation processes, (iii) surface reactions and (iv) degradation processes. It remains to be seen whether such non-linear effects can be treated effectively in terms of frequency-dependent Warburg diffusion phenomena which, themselves, may be a special case of exponential or power law behaviour that can be represented by inclusion of CPEs in ECMs. At present, the research themes of non-linearity, diffusion phenomena, TLMs and CPEs are usually pursued separately but they may have a common origin.

An important point, irrespective of the data analysis procedure that is adopted, is to assess whether EIS data change during measurements and if so, because of either non-linearity or non-stationarity [9,28]. These effects may show up as either non-reproducibility of current-voltage Lissajous plots as breakdown of Kramers-Kronig compatibility between real and imaginary impedance components over a range of frequencies or as evidence of irreversible changes to the nature of a sample or cell as a result of EIS measurements.

Several recent papers discuss EIS presentation using both ECMs [29-31] and DRT [25]. A simple ECM that represents an ideal cell system with electrolyte resistance R_Ω, two electrode-electrolyte interfaces and an electrode diffusion Warburg is shown in Fig.3 (a), together with the ideal impedance representation in (b), the spectroscopic capacitance plot C' in (c) and the calculated DRT in (d). The Warburg is connected in series with the charge transfer component shown in Fig.2(c), bottom. An alternative ECM may be chosen in which the Warburg is connected as shown in Randles' circuit, Fig.2(c), top. The specific parameter values used in Fig.(3) simulation give very similar results in both models. Thus, with decreasing frequency, or increasing time constants, the main features that appear in a LIB are suggested to be: ohmic resistance; solid-electrolyte interphases (SEIs); charge transfer (CT); bulk Li diffusion through the electrode(s) [25,29,30]. The different phenomena in LIBs or sodium-ion batteries (SIBs) are therefore separated according to their time constants which, in many cell construction conditions, may be related directly to their associated capacitances. A good correlation between DRT peaks and the ECM is seen for the higher frequency components, Fig.3(b),(d), but the DRT is unable to simulate the frequency dependence of the low frequency Warburg element and instead, gives multiple peaks.

This illustrates the risk that DRT analysis may give separate peaks that do not correspond to elements of the ECM and may be an artefact of the DRT procedure.

EIS studies are not usually carried out in isolation, but together with other electrochemical or materials characterisation techniques, give improved understanding of the factors that influence battery performance [32-34].

Na ion batteries and cell components

i) Na solid electrolytes

Na batteries have been under development for over 60 years following the discovery of high levels of Na^+ ion conductivity in Na beta alumina [35]. This forms as a by-product of the glass industry and is found in the refractory alumina bricks used to line glass melting furnaces. The Na beta-alumina, of approximate composition $Na_2O{\cdot}(5\text{-}11)Al_2O_3$, developed by reaction of Na^+ ions from the glass melt with the alumina lining and was found to exhibit very high levels of Na^+ ion conductivity, ~ 30 mS cm^{-1} at 25 °C with activation energy 0.16(1) eV.

There are two well-established polymorphs of beta-alumina, β and β'', both have layered structures but differ in their layer stacking sequence and details of the Na^+ ion conduction pathway. The β'' form has the highest conductivity above room temperature and is usually preferred for applications as a solid electrolyte. It shows a disordering transition of the Na^+ ions and a curved conductivity Arrhenius plot whereas the β form shows remarkably linear Arrhenius behaviour over the entire temperature range -180 to 1000 °C. Na beta-aluminas still have the highest conductivity of Na^+ ions reported

in a ceramic at room temperature. Their ionic conduction is only two dimensional because the mobile Na^+ ions reside in open layers, or 'conduction planes', that are separated by impermeable 'spinel blocks'. Ceramics have somewhat lower ionic conductivity than single crystals because the tortuous conduction pathway through a ceramic with randomly-oriented grains leads to a significant increase in effective conduction pathlength. Fortunately, grain boundary impedances are not usually significant in well-sintered beta-alumina ceramics.

This discovery of high ionic conduction at room temperature in beta-alumina ceramic, together with discovery of similar levels of Ag^+ ion conductivity in AgI at high temperatures and $RbAg_4I_5$ at room temperature, created great interest in novel battery designs that used solid electrolytes instead of the conventional liquid electrolytes. It also led to creation of the Solid State Ionics research discipline. Around the same time, conductivity measurements evolved from fixed frequency measurements using manual bridges into the now-familiar broadband IS technique, illustrated by the stand-out publication of Bauerle on admittance spectroscopy of stabilised zirconia oxide ion conductors [36].

Impedance measurements on single crystal Na beta-alumina with solid Au electrodes showed an example of a perfect double layer blocking capacitance with a 90° electrode spike in impedance complex plane plots [37], thereby confirming the absence of any electronic conductivity. It was subsequently shown that the surface of the crystal had very low conductivity and contained no mobile Na^+ ions [38]. This was an early indication of potential additional impedances that may arise at solid-solid interfaces in all-solid-state batteries (ASBs).

Measurements on single crystal Na beta-alumina showed very strong departures from ideal Debye-like behaviour of the bulk impedance and were characterised by Jonscher power law response at high frequencies. This indicated that non-ideality of impedance data, and its possible representation by a CPE, is likely to be a common feature of homogeneous, single phase, ionically-conducting materials [39]. It is attributable to details of the conduction mechanism and specifically to co-operative interactions between mobile charge carriers. In the case of Debye-like behaviour, the mobile species move independently of their surroundings and should exhibit a resistance that is frequency-independent. With a high concentration of mobile carriers, however, as in beta-alumina, ionic interactions between Na^+ ions, and with the lattice oxide ions lead to creation of ion atmospheres, a well-known feature of liquid electrolytes, that act as a drag on long range conduction and give rise to frequency-dependent resistances.

Na beta-alumina ceramics formed the basis for development of Na-S high temperature (300 to 350 °C) batteries which had the inverse design of a solid electrolyte between molten sodium and sulfur electrodes [40]. These batteries reached the level of commercialisation for megawatt power station load levelling in Japan and prototype electric vehicles in various other countries. A similar battery configuration using beta-alumina solid electrolyte is the Zebra cell, Na/beta-alumina/$NaAlCl_4$ [41].

Alternative Na^+ solid electrolytes to beta-alumina have been developed, particularly, the 'Nasicon' family based on $Na_3Zr_2Si_2PO_{12}$ [42,43]. High Na^+ ion conductivity arises in e.g. $Na_{3.1}Zr_{1.55}Si_{2.3}P_{0.7}O_{11}$ by varying the Si:P ratio, and reducing Zr content to avoid precipitation of zirconia, together with changes of Na^+ content to maintain charge balance [44]. Research into new NASICONs continues, with e.g. a room temperature conductivity of 2.74×10^{-3} $S\cdot cm^{-1}$ reported for a Zn-doped composition [45] and with their potential use as the electrolyte in ASBs [44,45]. Recent progress in NASICONs as well as other inorganic electrolytes for ASBs is reviewed in [46].

ii) SEI and CEI

One of the most important, but probably least-well understood, contributions to the operation, cycling and lifetimes of batteries concerns the solid electrolyte interfaces and interphases SEI, that form on contact between the electrolyte and electrodes [47]. In almost all publications, the term SEI refers to the anode SEI and unless stated specifically, it refers to the region that may include either, or both, interface and interphase. The anode SEI appears to be a protective layer that inhibits further reaction between anode and electrolyte but is also an ionically conductive membrane that facilitates charge transfer between them. The role of any cathode SEI is less well understood and may arise from reaction of electrolyte with the cathode when it is in a high state of charge.

It is expected that SEIs would contribute to overall cell impedances but as yet, definitive EIS studies of their development and significance appear not to have been made for Na batteries. The decoupling of SEI resistance from ionic diffusion associated with electrode porosity in Li batteries has been demonstrated and simulated using a transmission line model [48]. The spatial arrangement of the constituent material phases that form a porous electrode affect correlation between electrochemical behaviour and ionic transport within the electrode [49]. The use of EIS to show the influence of layer-by-layer SEI in battery performance has been shown [50]. It was suggested that the solubility of an Na-based SEI in $NaPF_6$, EC/DEC electrolyte is a major factor leading to self-discharge compared with that of the less soluble Li analogue [51]. The trade-off between formation of a thin SEI film and desolvation of Na at the carbon interface, both of which impact on battery performance, has been demonstrated [33]. Na dendrite growth resulting from side reactions with electrolyte was shown to reduce in the presence of a thin Ag layer at the sodium metal surface [52]. Monte Carlo modelling has been used to gain molecular-scale insight into the phenomena that influence SEI growth, its subsequent behaviour and dissolution, in support of experimental results and general understanding of SEIs [53]. An alternative approach to study SEIs has been to deliberately fabricate them; a range of artificial SEI interfaces has been reviewed [54].

The formation, stability and nature of cathode-electrolyte interfaces (CEI) for SIBs has been reviewed [55]. As yet, an overall picture of CEI formation and analysis

methodology is absent in the literature but future developments are anticipated with increasing interest in high energy battery technologies [56,57].

iii) Anode

The preferred anode for many SIBs is based on 'hard carbon' because graphitic carbons that work well with Li batteries give only limited intercalation possibilities with Na; for solid state Na batteries, alloy anodes may be advantageous [58]. EIS measurements on Na storage in hard carbon-like materials were processed to give DRT profiles [59]. During initial Na intercalation characterised by a sloping voltage dependence, the change in DRT profile was attributed to the dominant effect of mass diffusion on overall resistance. In the subsequent voltage plateau region, mass diffusion was no longer rate controlling and the DRT profile was unchanged; finally, at the latest stage of charge, the profile changed again and was attributed to Na electroplating. The structural features of hard carbon and its sodium storage capabilities have been reviewed [60,61] and two key factors identified, the pore structure and the presence of surface functional groups [61]. Biomass-derived carbons showed correlations between the microcrystalline structure, electrochemical performance and the biomass carbonization temperature [62]. It was shown by ^{23}Na NMR and other studies that Na ions store initially at defects within interlayers and at pore surfaces of hard carbons; subsequently, sodium clusters with some evidence of metallicity form during a low voltage plateau region [63].

iv) Cathode

The layered transition metal oxides, Na_xTMO_2 are currently a preferred option for rechargeable Na batteries due to their high specific capacity and high voltage, but several phase transitions occur during cycling leading to poor understanding of the mechanistic details during cell operation. Impedance studies fall into two groups, involving measurements of the conductivity of the materials in isolation and electrode studies containing a composite cathode with conducting carbon additive. Improved transport properties of a P2-type transition metal oxide led to enhanced interfacial kinetics of sodium ion transfer at the interface, thereby exhibiting better rate performance in cells [64]. A combined study of EIS using 3-terminal measurements, ECM and DRT enabled separation of impedance of a O3-type layered transition metal cathode at different frequencies and potentials and identified a significant influence of phase transitions during cycling on CT processes [65].

Summary

EIS of electrochemical systems continues to be a rapidly expanding topic with a combination of new materials, improved data analysis procedures that include modelling or simulations and greater understanding of correlations between cell design, materials microstructure and impedance response. Use of DRT analysis to complement equivalent circuit modelling may have a useful role to play but as yet, the

non-ideal behaviour of real impedance data represents a barrier to its successful implementation.

Acknowledgement
ARW thanks the Faraday Institution, grant FIRG017 and EPSRC, grant EP/X040305/1 for financial support.

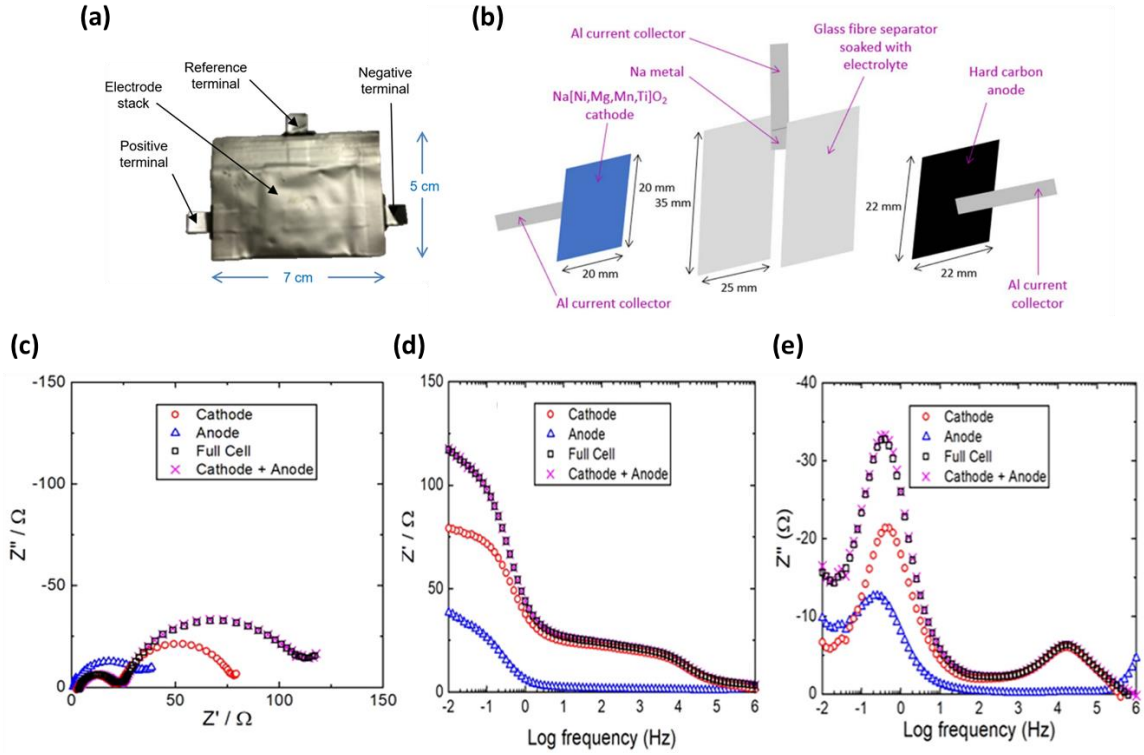

Fig.1(a)(b). Three-electrode pouch cell design for an in-house constructed sodium-ion battery. Three-electrode EIS data: (c) impedance complex plane plots, (d,e) spectroscopic plots of Z' and Z''. Full cell data match very well the summed data of cathode and anode components. Adapted from [4].

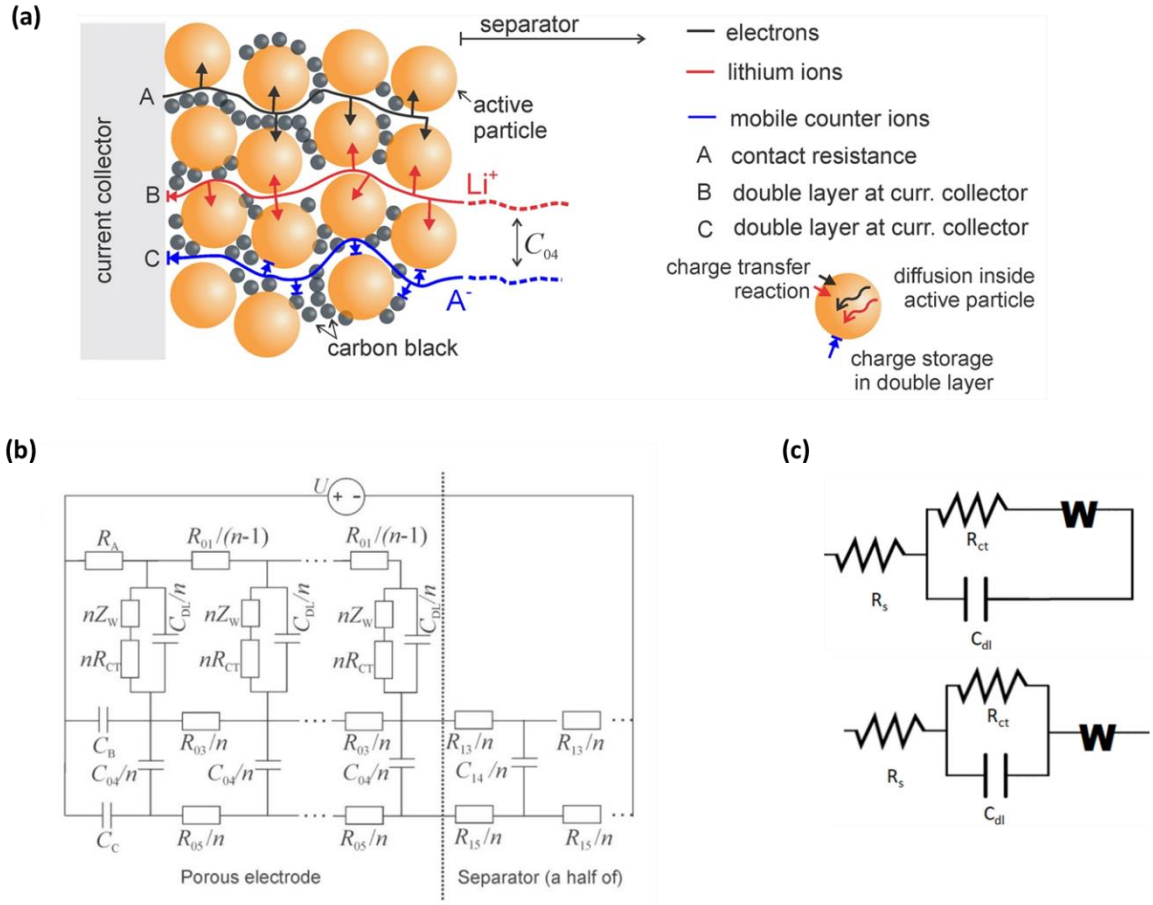

Fig.2. (a) Schematics showing the movement of electrons and mobile ions in a typical Li-ion insertion positive electrode. (b) Transmission line model applicable to the processes in (a). Adapted from [16]. (c) Top: Randles circuit where the series-connected Warburg element and the charge transfer resistance are in parallel with the double layer capacitance. Bottom: The parallel-connected charge transfer resistance and double layer capacitance are in series with the Warburg element. R_s represents the electrolyte resistance. Adapted from [18].

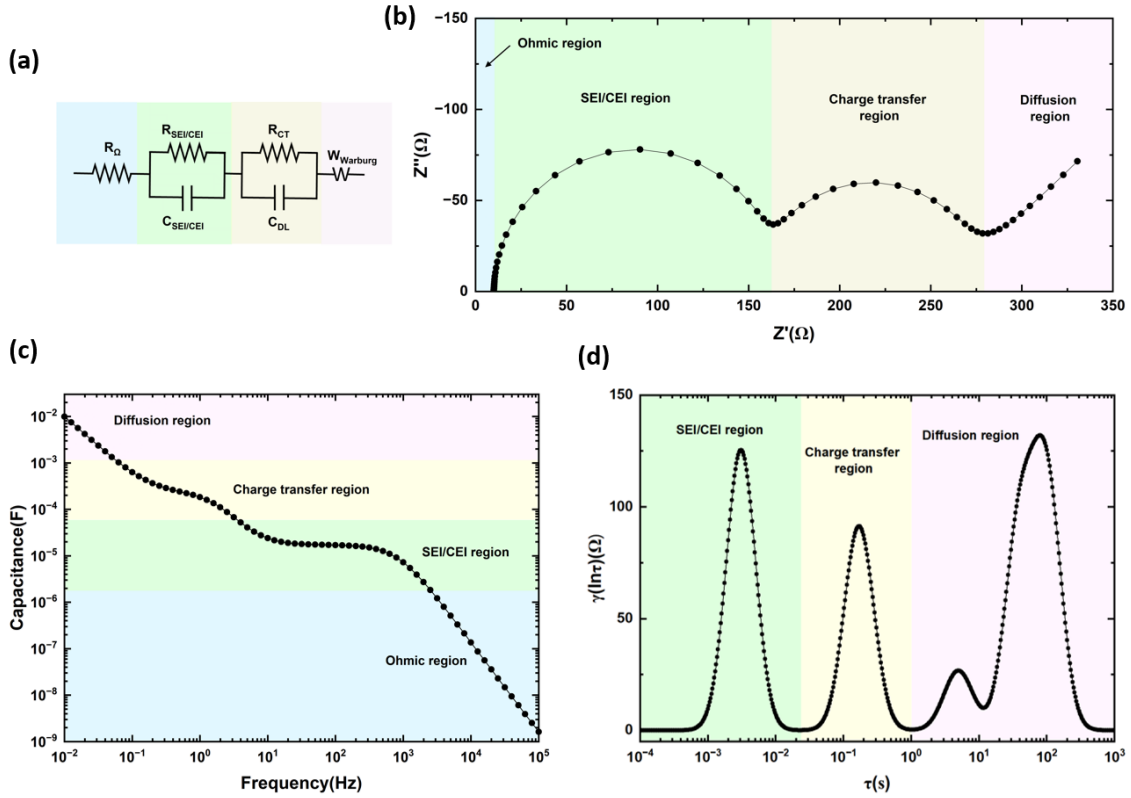

Fig.3. (a) ECM showing four series-connected circuit elements with simulated (b) impedance complex plane, (c) capacitance, C' spectroscopic plot, (d) DRT. The different features labelled in (b-d) correspond to the circuit elements in (a). Data used for the simulations were R_Ω = 10 Ω, $R_{SEI/CEI}$ = 150 Ω, $C_{SEI/CEI}$ = 20 μF, R_{CT} = 100 Ω, C_{CT} = 1.5 mF, σ_W = 17.68 $\Omega s^{-1/2}$, frequency range from 10 mHz to 100 kHz, produced by Zview software. A Matlab toolbox DRTtools was used for computing DRT [66]; A Gaussian basic function was used for discretization; the regularization parameter λ was set to 0.001, the FWHM parameter was set to 0.2.

References

1. Yan Z: **Symmetric Cells as an Analytical Tool for Battery Research: Assembly, Operation, and Data Analysis Strategies**. *Journal of The Electrochemical Society* 2023, **170**:020521.

2. Ender M, Weber A, Ellen I-T: **Analysis of Three-Electrode Setups for AC-Impedance Measurements on Lithium-Ion Cells by FEM simulations**. *Journal of The Electrochemical Society* 2011, **159**:A128.

3. Middlemiss LA, Rennie AJR, Sayers R, West AR: **Use of Three-Terminal Impedance Spectroscopy to Characterize Sodium-Ion Batteries at Various Stages of Cycle Life**. *Journal of The Electrochemical Society* 2024, **171**:010528.

4. Middlemiss LA, Rennie AJR, Sayers R, West AR: **Characterisation of batteries by electrochemical impedance spectroscopy**. *Energy Reports* 2020, **6**:232-241.

5. Ma H, Sinclair DC, Dean JS: **A finite element study on the influence of surface cracks on micro-contact impedance spectroscopy measurements**. *Solid State Ionics* 2023, **393**:116173.

6. Ma H, Sinclair DC, Dean JS: **Modifications to the spreading resistance equation when using micro-contact impedance spectroscopy to measure resistive surface layers**. *Solid State Ionics* 2024, **414**:116652.

7. Cooper SJ, Bertei A, Finegan DP, Brandon NP: **Simulated impedance of diffusion in porous media**. *Electrochimica Acta* 2017, **251**:681-689.

8. Nguyen T-T, Demortière A, Fleutot B, Delobel B, Delacourt C, Cooper S, J: **The electrode tortuosity factor: why the conventional tortuosity factor is not well suited for quantifying transport in porous Li-ion battery electrodes and what to use instead**. *npj Computational Materials* 2020, **6**:123.

9. Lopez-Richard V, Pradhan S, Wengenroth Silva RS, Lipan O, Castelano LK, Höfling S, Hartmann F: **Beyond equivalent circuit representations in nonlinear systems with inherent memory**. *Journal of Applied Physics* 2024, **136**:165103.

10. Thapa A, Gao H: **Low-frequency Inductive Loop and Its Origin in the Impedance Spectrum of a Graphite Anode**. *Journal of The Electrochemical Society* 2022, **169**:110535.

11. Li C, Peng Z, Huang J: **Impedance Response of Electrochemical Interfaces: Part IV—Low-Frequency Inductive Loop for a Single-Electron Reaction**. *The Journal of Physical Chemistry C* 2023, **127**:16367-16373.

12. Komar A, Wilmer D, Wilkening HMR, Hanzu I: **Accounting for stray capacitances in impedance measuring cells — A mandatory step in the investigation of solid ion conductors**. *Solid State Ionics* 2023, **393**:116169.

13. Ramírez-González J, Sinclair DC, West AR: **Impedance and Dielectric Spectroscopy of Functional Materials: A Critical Evaluation of the Two Techniques**. *Journal of The Electrochemical Society* 2023, **170**:116504.

14. McKubre MCH, Macdonald DD, Sayers B, Macdonald JR: **Measuring Techniques and Data Analysis**. In *Impedance Spectroscopy*. Edited by; 2018:107-174.

15. Hernández MA, Masó N, West AR: **On the correct choice of equivalent circuit for fitting bulk impedance data of ionic/electronic conductors**. *Applied Physics Letters* 2016, **108**:152901.

16. Moškon J, Gaberšček M: **Transmission line models for evaluation of impedance response of insertion battery electrodes and cells**. *Journal of Power Sources Advances* 2021, **7**:100047.

17. Bumberger AE, Nenning A, Fleig J: **Transmission line revisited – the impedance of mixed ionic and electronic conductors**. *Physical Chemistry Chemical Physics* 2024, **26**:15068-15089.

18. Orazem ME, Ulgut B: **On the Proper Use of a Warburg Impedance**. *Journal of The Electrochemical Society* 2024, **171**:040526.

19. Randles JEB: **Kinetics of rapid electrode reactions**. *Discussions of the Faraday Society* 1947, **1**:11-19.

20. Jonscher AK: **The 'universal' dielectric response**. *Nature* 1977, **267**:673-679.

21. Almond DP, Bowen CR: **Anomalous Power Law Dispersions in ac Conductivity and Permittivity Shown to be Characteristics of Microstructural Electrical Networks**. *Physical Review Letters* 2004, **92**:157601.

22. Vainas B, Almond DP, Luo J, Stevens R: **An evaluation of random R-C networks for modelling the bulk ac electrical response of ionic conductors**. *Solid State Ionics* 1999, **126**:65-80.

23. Lu Y, Zhao C-Z, Huang J-Q, Zhang Q: **The timescale identification decoupling complicated kinetic processes in lithium batteries**. *Joule* 2022, **6**:1172-1198.

24. Maradesa A, Py B, Huang J, Lu Y, Iurilli P, Mrozinski A, Law HM, Wang Y, Wang Z, Li J, et al.: **Advancing electrochemical impedance analysis through innovations in the distribution of relaxation times method**. *Joule* 2024, **8**:1958-1981.

25*. Sohaib M, Akram AS, Choi W: **Analysis of Aging and Degradation in Lithium Batteries Using Distribution of Relaxation Time**. *Batteries (Basel)* 2025, **11**:34.

Use of DRT method effectively separates overlapping electrochemical processes in Nyquist plots. Clear shifts in peak positions attributable to processes such as charge transfer and diffusion correlate with the degradation of LIBs over time.

26. DiGiuseppe G, Hunter A, Zhu F: **Combined equivalent circuits and distribution of relaxation times analysis and interfacial effects of $(La_{0.60}Sr_{0.40})_{0.95}Co_{0.20}Fe_{0.80}O_{3-x}$ cathodes**. *Electrochimica Acta* 2020, **350**:136252.

27. Bakenhaster ST, Dewald HD: **Electrochemical impedance spectroscopy and battery systems: past work, current research, and future opportunities**. *Journal of Applied Electrochemistry* 2025, **55**:1657-1681.

28*. Zabara MA, Goh JM, Gaudio VM, Zou L, Orazem ME, Ulgut B: **Utility of Lissajous Plots for Electrochemical Impedance Spectroscopy Measurements: Detection of Non-Linearity and Non-Stationarity**. *Journal of The Electrochemical Society* 2024, **171**:010507.

The value of current-potential Lissajous plots is highlighted as a means to evaluate sample changes during the EIS measurement procedure using data obtained variously from a $LiFePO_4$ secondary battery, a $LiSOCl_2$ primary battery, a 350 F supercapacitor and a stainless steel rod immersed in an electrolyte.

29. Choi W, Shin H-C, Kim JM, Choi JY, Yoon WS: **Modeling and Applications of Electrochemical Impedance Spectroscopy (EIS) for Lithium-ion Batteries**. *Journal of Electrochemical Science and Technology* 2020, **11(1)**:1-13.

30. Haeverbeke MV, Stock M, Baets BD: **Equivalent Electrical Circuits and Their Use Across Electrochemical Impedance Spectroscopy Application Domains**. *IEEE Access* 2022, **10**:51363-51379.

31. Laschuk NO, Easton EB, Zenkina OV: **Reducing the resistance for the use of electrochemical impedance spectroscopy analysis in materials chemistry**. *RSC Advances* 2021, **11**:27925-27936.

32. Stolz L, Gaberšček M, Winter M, Kasnatscheew J: **Different Efforts but Similar Insights in Battery R&D: Electrochemical Impedance Spectroscopy vs Galvanostatic (Constant Current) Technique**. *Chemistry of Materials* 2022, **34**:10272-10278.

33. Liu M, Jiang Z, Wu X, Liu F, Li W, Meng D, Wei A, Nie P, Zhang W, Zheng W: **Reinventing the High-rate Energy Storage of Hard Carbon: the Order-degree Governs the Trade-off of Desolvation-Solid Electrolyte Interphase at Interfaces**. *Angewandte Chemie International Edition* 2025, **64**:e202425507.

34. Zoric MR, Fabbri E, Herranz J, Schmidt TJ: **In Situ and Operando Spectroscopic Techniques for Electrochemical Energy Storage and Conversion Applications**. *The Journal of Physical Chemistry C* 2024, **128**:19055-19070.

35. Yung-Fang Yu Y, Kummer JT: **Ion exchange properties of and rates of ionic diffusion in beta-alumina**. *Journal of Inorganic and Nuclear Chemistry* 1967, **29**:2453-2475.

36. Bauerle JE: **Study of solid electrolyte polarization by a complex admittance method**. *Journal of Physics and Chemistry of Solids* 1969, **30**:2657-2670.

37. Armstrong RD, Firman RE, Thirsk HR: **The a.c. impedance of complex electrochemical reactions**. *Faraday Discussions of the Chemical Society* 1973, **56**:244-263.

38. Hunter CC, Ingram MD, West AR: **A.C. impedance of surface layers and blocking electrodes on single crystal ß-alumina**. *Journal of Materials Science Letters* 1982, **1**:522-524.

39. Grant RJ, Hodge IM, Ingram MD, West AR: **Conductivity dispersion in single-crystal β-alumina electrolyte**. *Nature* 1977, **266**:42-43.

40. Wen Z, Hu Y, Wu X, Han J, Gu Z: **Main Challenges for High Performance NAS Battery: Materials and Interfaces**. *Advanced Functional Materials* 2013, **23**:1005-1018.

41. Sudworth JL: **The sodium/nickel chloride (ZEBRA) battery**. *Journal of Power Sources* 2001, **100**:149-163.

42. Goodenough JB, Hong HYP, Kafalas JA: **Fast Na+-ion transport in skeleton structures**. *Materials Research Bulletin* 1976, **11**:203-220.

43. Hong HYP: **Crystal structures and crystal chemistry in the system $Na_{1+x}Zr_2Si_xP_{3-x}O_{12}$**. *Materials Research Bulletin* 1976, **11**:173-182.

44. Go W, Kim J, Pyo J, Wolfenstine JB, Kim Y: **Investigation on the Structure and Properties of $Na_{3.1}Zr_{1.55}Si_{2.3}P_{0.7}O_{11}$ as a Solid Electrolyte and Its Application in a Seawater Battery**. *ACS Appl Mater Interfaces* 2021, **13**:52727-52735.

45. Park G, Jeon DW, Jang I-S, Ahn B-J, Baek K, Song B-Y, Kim E-h, Bang J, Kang YC, Cho SB, et al.: **Investigation of the effects of heteroatom doping on von-Alpen-type NASICON electrolytes and its applications to solid-state sodium batteries**. *Journal of Advanced Ceramics* 2025, **14**:9221138.

46. Radjendirane AC, Maurya DK, Ren J, Hou H, Algadi H, Xu BB, Guo Z, Angaiah S: **Overview of Inorganic Electrolytes for All-Solid-State Sodium Batteries**. *Langmuir* 2024, **40**:16690-16712.

47. Villevieille C: **The challenge of studying interfaces in battery materials**. *Nature Nanotechnology* 2025, **20**:2-5.

48. Lin J, Hu W, Yang J, Pan L, Xia X, Wei Y, Gong Z, Yang Y: **Revisiting High-Frequency Impedance in Li-Ion Batteries: Decoupling Solid Electrolyte Interphase Resistance from Pore Impedance**. *The Journal of Physical Chemistry Letters* 2025, **16**:7490-7497.

49. Mistry AN, Mukherjee PP: **Probing spatial coupling of resistive modes in porous intercalation electrodes through impedance spectroscopy**. *Physical Chemistry Chemical Physics* 2019, **21**:3805-3813.

50. Ma M, Cai H, Xu C, Huang R, Wang S, Pan H, Hu YS: **Engineering Solid Electrolyte Interface at Nano-Scale for High-Performance Hard Carbon in Sodium-Ion Batteries**. *Advanced Functional Materials* 2021, **31**:2100278.

51. Mogensen R, Brandell D, Younesi R: **Solubility of the Solid Electrolyte Interphase (SEI) in Sodium Ion Batteries**. *ACS Energy Letters* 2016, **1**:1173-1178.

52**. Zhang W, Lu Q, Sun G, Chen Z, Yue P, Zhang G, Song B, Song K: **Sodiophilic Interface Induces a NaF-Rich Solid Electrolyte Interface for Stable Sodium-Metal Batteries under Harsh Conditions**. *Nano Lett* 2025, **25**:6092-6100.

The problem of dendritic growth at Na/electrolyte interface for Na-metal batteries is treated by Ag coating, leading to uniform Na deposition. This is attributed to strong Na/Ag interaction and a NaF-rich SEI.

53. Hankins K, Putra MH, Wagner-Henke J, Groß A, Krewer U: **Insights on SEI Growth and Properties in Na-Ion Batteries via Physically Driven Kinetic Monte Carlo Model**. *Advanced Energy Materials* 2024, 2401153.

54. Gao Y, Yao Y, Shi P, Huang F, Jiang Y, Yu Y: **Advanced Interphases Layers for Dendrite-Free Sodium Metal Anodes**. *ACS Applied Materials & Interfaces* 2025, **17**:17881-17894.

55. Zhang J, Ma S, Zhang J, Zhang J, Wang X, Wen L, Tang G, Hu M, Wang E, Chen W: **Critical review on cathode electrolyte interphase towards stabilization for sodium-ion batteries**. *Nano Energy* 2024, **128**:109814.

56. Xiao J, Adelstein N, Bi Y, Bian W, Cabana J, Cobb CL, Cui Y, Dillon SJ, Doeff MM, Islam SM, et al.: **Assessing cathode–electrolyte interphases in batteries**. *Nature Energy* 2024, **9**:1463-1473.

57. Zhang N, Wang B, Jin F, Chen Y, Jiang Y, Bao C, Tian J, Wang J, Xu R, Li Y, et al.: **Modified cathode-electrolyte interphase toward high-performance batteries**. *Cell Reports Physical Science* 2022, **3**:101197.

58*. Yu X, Chen S, Tang B, Li X-L, Zhou J, Ren Y, Wei J, Yang C, Guo Y, Zhou Z, et al.: **The Debate over Hard Carbon and Alloy Anodes Continues for Solid-State Sodium Batteries**. *ACS Energy Letters* 2024, **9**:4441-4449.

Comparison of hard carbon and alloy anodes for solid state sodium batteries and the nature of the electrical double layer.

59. Schutjajew K, Tichter T, Schneider J, Antonietti M, Roth C, Oschatz M: **Insights into the sodiation mechanism of hard carbon-like materials from electrochemical impedance spectroscopy**. *Physical chemistry chemical physics : PCCP* 2021, **23**:11488-11115.

60. Chen S, Hu T, Yu T, Luo X, Zhang L, Li F: **Structural Feature Design for Carbon Materials toward Sodium Storage: Insights and Prospects**. *ACS Energy Letters* 2025, **10**:1931-1952.

61. Xu L, Li Y, Xiang Y, Li C, Zhu H, Li C, Zou G, Hou H, Ji X: **Bridging Structure and Performance: Decoding Sodium Storage in Hard Carbon Anodes**. *ACS Nano* 2025, **19**:14627-14651.

62. Li Y: **Unveiling structure-activity relationship between carbon crystallography and sodium ion battery anodes**. *Solid State Communications* 2025, **401**:115933.

63. Au H, Alptekin H, Jensen ACS, Olsson E, O'Keefe CA, Smith T, Crespo-Ribadeneyra M, Headen TF, Grey CP, Cai Q, et al.: **A revised mechanistic model for sodium insertion in hard carbons**. *Energy & Environmental Science* 2020, **13**:3469-3479.

64. Shanmugam R, Lai W: **Study of Transport Properties and Interfacial Kinetics of $Na_{2/3}[Ni_{1/3}Mn_xTi_{2/3-x}]O_2$ (x = 0,1/3) as Electrodes for Na-Ion Batteries**. *Journal of The Electrochemical Society* 2015, **162**:A8.

65. Li M, Qiu X, Wei T, Dai Z: **Study of Predominant Dynamics on the O3-Type Layered Transition-Metal Oxide Cathode by Electrochemical Impedance Spectroscopy for Sodium-Ion Batteries**. *Langmuir* 2023, **39**:8865-8878.

66. Wan TH, Saccoccio M, Chen C, Ciucci F: **Influence of the Discretization Methods on the Distribution of Relaxation Times Deconvolution: Implementing Radial Basis Functions with DRTtools**. *Electrochimica Acta* 2015, **184**:483-499.